Military Technical College
Kobry El-Kobbah,
Cairo, Egypt

14th International Conference on Applied Mechanics and Mechanical Engineering.

Experimental investigation of electron beam welding of AA1350 aluminum alloy

By

Zuhair Agab Elseddig * M. Sobih ** Kh. Almazy ** M. T.Sallam **

Abstract:

Aluminum's unique properties, *e.g.* light weight, high strength, and resistance to corrosion, make it an ideal material for use in conventional and novel applications. Aluminum has become increasingly used in the production of aerospace equipment, automobiles and trucks, packaging of food and beverages. However it suffers from poor joint strength when welded by conventional fusion welding. In this investigation an attempt has been made to improve the welded joint strength through using of electron beam welding (EBW). Due to special features of EBW, *e.g*. high energy density and accurately controllable beam size and location, in many cases it has proven to be an efficient method for joining difficult to weld materials. In this paper, the effects of EBW parameters on the ultimate tensile strength (UTS) has been investigated, The experiments were based on one-variable-at-a-time (OVAT) method,

Keywords:

Aluminum alloy welding, Electron beam welding, one-variable-at-a-time, Tensile strength

* Sudanese armed forces
** Egyptian armed forces

1. Introduction:

The properties of Aluminum alloys, *viz*. high thermal conductivity, high strength, good formability and low weight, made it considerable for aerospace structure, shipbuilding, cars manufacturing, *etc*. [1]. However there are many problems associated with welding of aluminum and its alloys that make it difficult to weld by conventional process. Conventional aluminum weld joints are characterized by the following defects: gas porosity; oxide inclusions; solidification cracking (hot tearing); reduced strength in both the weld and heat affected zone (HAZ); lack of fusion; reduced corrosion resistance; and reduced electrical resistance [2].

Welding processes such as friction stir welding; gas metal arc welding (MIG); and electron beam welding (EBW) are adopted for joining aluminum components [3]. The high power density associated with the electron beam (EB) and the ability to work in a vacuum environment make it possible to use the process for joining metals which not only have high melting points but also those which are extremely reactive when hot or molten [4]. Aluminum and many of its alloys can be welded readily using the EB process without the danger of oxidation and subsequent undetectable degradation of ductility. For this reason, the process is used widely in the aero engine industry for welding aluminum alloy parts [5].

Improper selection of process parameter causes defects in the fusion zone (FZ) of weldments, which could seriously influence the weld mechanical properties. Presently, there have been only a few studies on EBW of aluminum and its alloys [6-8], which is generally due to the high cost of EBW equipment for academic research. Welding quality is strongly determined by mechanical properties of the welded joints. Therefore, the selection of the welding process parameters is very essential for obtaining optimal tensile strength.
There are several approaches which can be used to investigate the effects of different testing parameters, such one-variable-at-a-time (OVAT) procedure, fractional factorial designs, and Taguchi method [9-11]. One of the common approaches employed by many engineers in manufacturing is (OVAT), where we vary one variable at a time keeping all other variables in the experiment fixed. Even though fractional factorial designs have well-known advantages over (OVAT) designs, the latter have several attractive features such as run size economy, continually receive information from each run rather than having to wait until the entire experiment is completed [12].
The most important input EBW parameters which would control the welding quality outputs are: beam current (Ib); sweep size (ss); welding speed (v); and focus position (If) [13]

The aim of this study is to investigate the effects of previously mentioned welding parameters on the ultimate tensile strength (UTS) as a welding output and considered as a response, and the prediction of the optimal combinations of the welding parameters with an objective of maximizing it. The experiments were based on (OVAT) method (four factors with three levels). Accordingly, 27 specimens of AA1350 aluminum alloy plate were welded in three sets each corresponds to different working distances (WD), and examined in a comparative study.

2. Experimental method:

The workpiece material is strain hardening AA1350 aluminum alloy with chemical composition and mechanical property shown in table 1 and table 2 respectively, this alloy has a relatively large Fe and Si content to promote solid solution strengthening. The presence of Fe and Si as an impurity element in 1350 aluminum alloy results in forming of $Al_{12}Fe_3Si$ or $Al_9Fe_2Si_2$ constituents at grain boundaries [3]. The size of each plate is (70×60×8mm).

The specimens were initially cut by hack saw and ground using 400, 600, grit emery paper to guarantee good surface finishing and the flatness of each faces at the same level before conducting the experiments, and oxide film was removed by wire brush and degreased with acetone.

Table 1 *chemical composition of AA 1350 aluminum alloy*

Materials used	Element (wt %)						
AA 1350 aluminum alloy	Si	Fe	Bi	Mn	Sn	Pb	other
	Al						
	0.134	0.377	0.01	0.015	0.0075	0.005	0.0515
	99.4						

Table 2 *Mechanical property of AA 1350 aluminum alloy*

Materials used	Mechanical property			
AA 1350 aluminum alloy	UTS(MPa)	yield strength (MPa)	Hardness HB	Elongation
	103.12	83	38	11%

Table 3. *EBW parameter for each set*

No		parameter	Level 1	Level 2	Level 3
Set I WD 100mm	1	Beam current (mA)	27	32	37
	2	Welding speed (mm/s)	4	7	10
	3	Focus current (mA) (focal position)	902	912	917
	4	Sweep size	0	10	20
Set II WD 200mm	1	Beam current (mA)	28	33	38
	2	Welding speed (mm/s)	4	7	10
	3	Focus current (mA) (focal position)	847	857	867
	4	Sweep size	0	5	10
Set III WD 300mm	1	Beam current (mA)	29	34	39
	2	Welding speed (mm/s)	4	7	10
	3	Focus current (mA) (focal position)	813	823	833
	4	Sweep size	0	3	6

A large number of trials have been conducted by try and error procedure to determine the working range of each factor, Absence of visible welding defects and at least half depth penetration were the criteria of choosing the working ranges. The levels for each factor were listed in table 3.

In this work, Seo TECH - 6O electron beam machine is used to conduct a series of experiments, the welding is done in the flowing sequence: the workpiece is loaded and fixed onto work-holding mechanism in welding chamber; then starting chamber pump down; after chamber has been reduced to 10^{-5}mbar the parameter was set to desired level and the beam was align to joint by using very low power beam spot; and then the welding operation has been conducted in auto mode.

After two plates welded together by a butt joint process the specimens for each run are prepared by cutting the plates 5mm away from the edge with cutoff wheel, the specimens are then cut into three samples, tensile test, impact tests , and metallographic observation, as shown in fig.1.

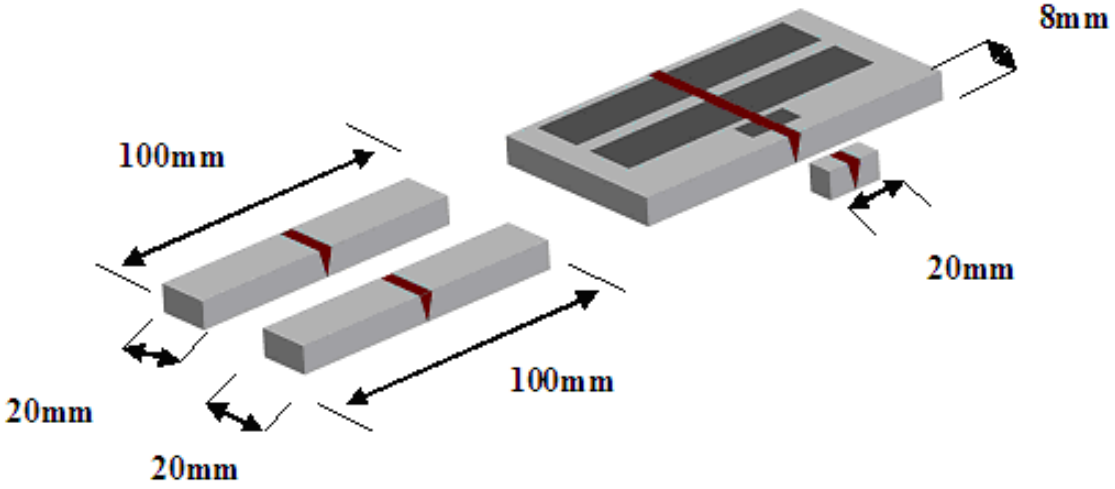

Figure (1). *Preparation of the AA1350 aluminum alloy samples for various inspection purposes*

Tensile test is conducted using Instron computer-controlled testing machine (model 8032). All the welded specimens are failed in the weld region, so the ultimate tensile strength of the specimens is the strength of the weld. Table 4 presents the lay out of this experiment, and the result of tensile test for each set.
Hardness test, impact test, and metallographic observation are done for two specimens with the highest and lowest UTS. Impact tests are measured by using charpy impact machine.

The hardness variation from the center of the fusion zone (FZ) across heat affected zone (HAZ) and to base metal (BM) is measured at an interval of 2 mm with an indenting load of 15.625kg by using Brinnell hardness testing machine, the position of hardness test are shown in Fig. 2(a) and the results are presented in Fig. 2(b).

Table 4 *result of tensile test*

	No	speed	Focus current	Beam current	Sweep size	UTS
Set I WD 100mm	1	4	912	32	0	36.54
	2	7	912	32	0	90.32
	3	10	912	32	0	82.5
	4	7	902	32	0	71.64
	5	7	922	32	0	64.197
	6	7	912	27	0	54.693
	7	7	912	37	0	59.787
	8	7	912	32	10	85.57
	9	7	912	32	20	80.6
Set II WD 200mm	1	4	857	33	0	55.557
	2	7	857	33	0	86.616
	3	10	857	33	0	66.645
	4	7	847	33	0	56.385
	5	7	867	33	0	62.442
	6	7	857	28	0	70.623
	7	7	857	38	0	81.243
	8	7	857	33	5	85.84
	9	7	857	33	10	70.749
Set III WD 300mm	1	4	823	34	0	80.64
	2	7	823	34	0	85.239
	3	10	823	34	0	59.787
	4	7	813	34	0	69.912
	5	7	833	34	0	65.871
	6	7	823	29	0	53.586
	7	7	823	39	0	79.632
	8	7	823	34	3	83.592
	9	7	823	34	6	55.314

Specimens for metallographic observation are suitably sectioned, mounted in transverse direction of the welding, mechanically polished according to standard metallographic procedures and etched using modified poulton reagent [50ml poulton reagent (60%HCl, 30%HNO_3, 5%HF, 5%H_2O), 25ml HNO_3, 40ml of solution of 1g chromic acid per 10ml of distilled water]. The etched samples are then placed under optical microscope to obtain a magnified image of the contours of penetration and HAZ.

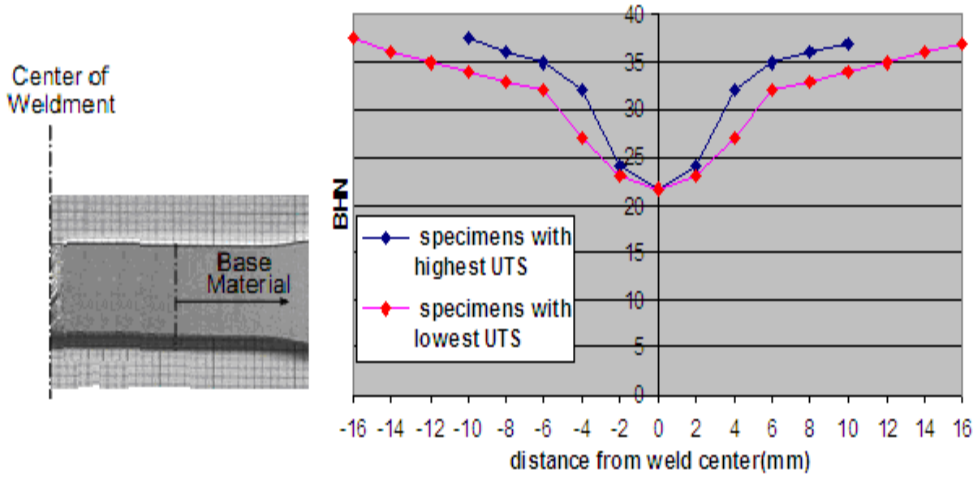

(a) *(b)*

Figure (2). *Hardness measurement as a function of position relative to the weld centreline*

3. Results and discussion.

Fig. 3 shows the microstructures of the highest UTS while Fig. 4 shows the microstructures of the lowest UTS weld.

The experiments of set-I produced better results as seen from Table 4 compared to set-II and set-III. So set-I only is considered in this discussion. The effects of the parameters on the output response for set-I are shown in Fig. 5, and can be summarize as follows.

• ***Weld speed:*** The effects of welding speed on the weldment strength are represented in Fig. 5(a). These results reveal that increasing welding speed increases the weldment strength to a max-value, and then further increase in welding speed decreases this strength. The weld bead obtained at low speed has a tear drop shape because of high heat input. As speed increases, heat input decreases and the weldment strength increases until an optimal value then decreases slightly due to the decrease in penetration depth. From experimental trials welding speed of 7mm/s has shown good results.

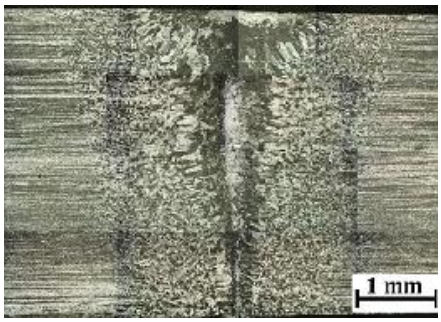

(a).

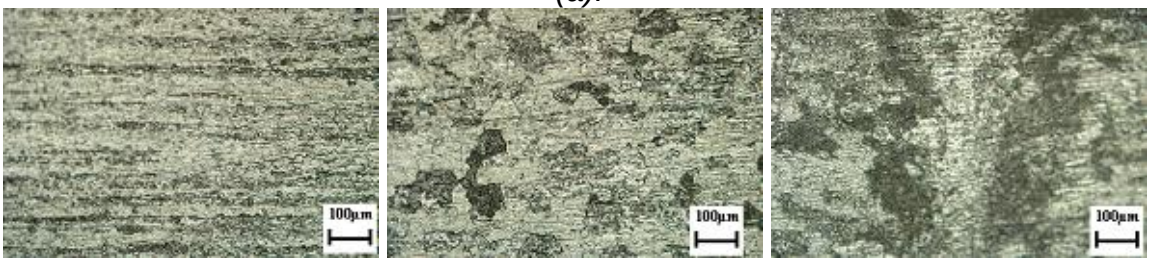

(b) *(c)* *(d)*

Figure (3): *Optical micrographs showing (a) fusion boundaries of the highest UTS sample, (b) microstructure of BM, (c) microstructure of HAZ, (d) microstructure of FZ*

Figure (4). *Optical micrographs showing fusion boundary of the worst sample*

• ***beam current:*** it was observed that as the beam current increases the UTS increases until an optimum value then decreases with any increase in beam current, Fig. 5(b), this can be explained by the increase in beam current leads to an increase in the heat input, this results in more penetration depth, and consequently higher UTS, however more increase in beam current leads to an increase of the amount of molten material, consequently the bead width increases and this decreases the UTS. From experimental trials beam current of 32 mA has shown the highest results.

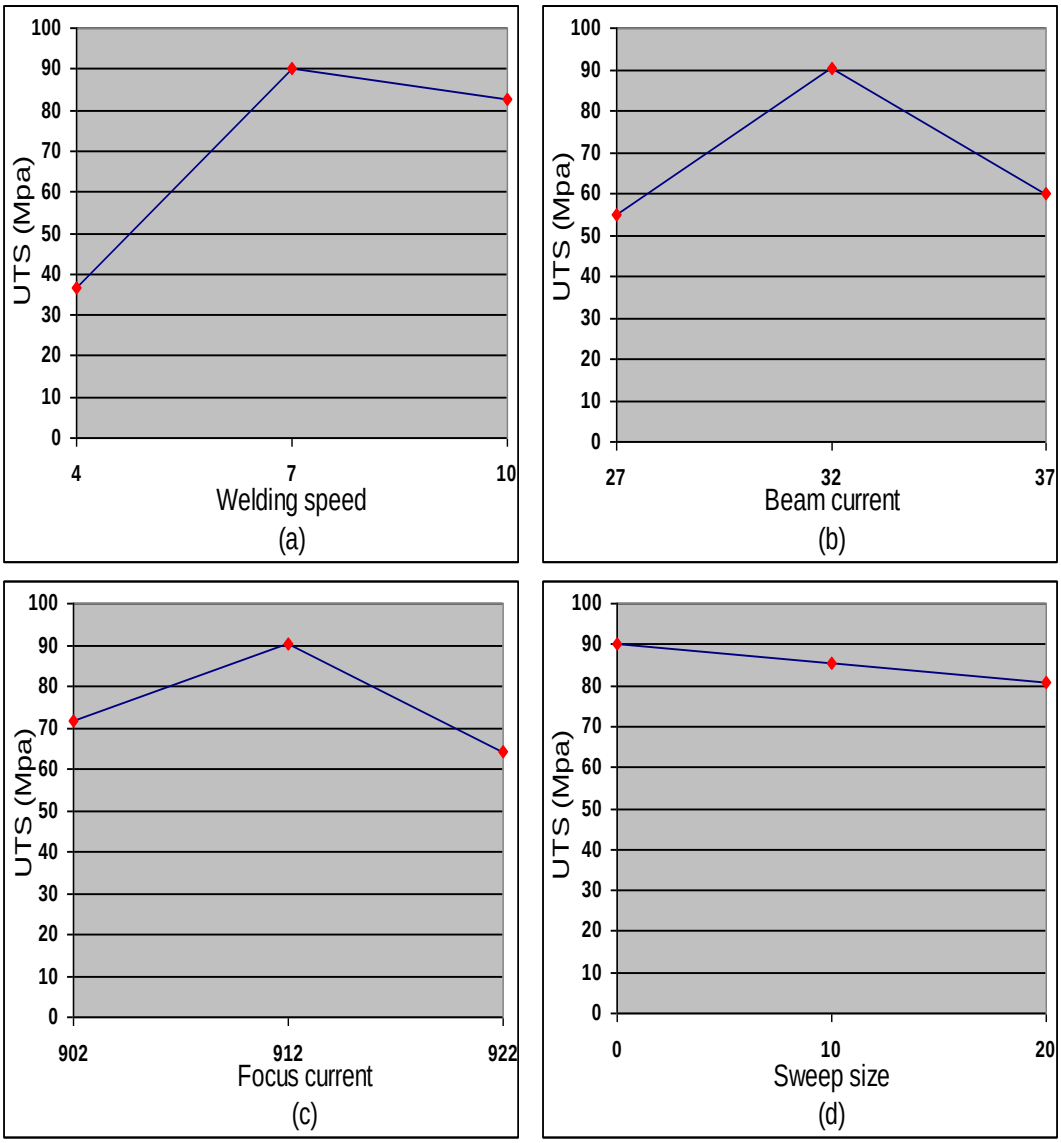

Figure (5). *effect of welding parameter on UTS, (a) effect of V when Ib,If,SS are fixed, (b) effect of Ib when, V,If,SS are fixed, (c) effect of If when, V,Ib,SS are fixed, (d) effect of SS when, V,Ib,If, are fixed,*

• ***Focus current (focal position):*** it was observed that weldment strength in the first stages increases as focus current is increased as shown in Fig. 5(c), focusing the electron beam (using If = 902mA) at the bottom of the welded specimen may lead to a substantial spreading of beam power onto wide area. Therefore, wide area of the base metal will melt; and hence, the weld pool exhibits shallow penetration and a large width/depth ratio so UTS decreases. When focusing beam current at the surface (using If = 922mA) penetration depth decreases and so UTS decreases, highest strength obtain when focusing beam current almost at the middle of the workpiece (using If = 912mA).

• ***Sweep size:*** as shown in Fig. 5(d), increasing the sweep size lead to an increase in the bead width and hence the weld strength decreases.

Impact tests showed that minimum value of absorbed energy were obtained in the specimens having lowest UTS (46.9 kJ/m^2), while in the highest UTS specimens a higher value (93.7kJ/m^2) was recorded. In the unwelded specimens (BM) the representative value is about120 kJ/m^2, thus exhibiting a remarkable reduction of toughness.

The base material has a brinnell hardness of about 38 BHN; however, the welding process softens the material significantly resulting in hardness reduction of nearly 50% around the weld line to about 22BHN. The variations in hardness can be readily correlated with the microstructure developed both during and after the welding process. It is most convenient to describe the microstructure in terms of the three main regions apparent in the hardness profiles; the unaffected parent material, Fig. 3(b), partially softened zone adjacent to the base metal (HAZ), Fig 3(c), and fully affected and softened region (FZ), Fig 3(d). Moreover a transition zone between them can be clearly visible. The parent microstructure which indicates that this material consists of long, thin grains, as stated earlier, the AA 1350 series alloys are work hardenable alloys and so this microstructure, typical of rolling work hardening, The recrystallisation of the parent microstructure can be seen in the (HAZ), Fig. 3(c) which shows small recrystallisation nuclei forming and growing on the grain boundaries of the original elongated microstructure. This (HAZ), is relatively narrow, on the other hand Fig .3(d) shows the microstructure of the softened region of the weld line (FZ). It can be seen that the welding process has dramatically altered the microstructure of the material in this region. The heavily worked microstructure of the base material has been completely replaced by a dendritic microstructure.

6. Conclusions:

In this study, the effects of the EBW parameters on weld strength using OVAT have been reported. The following points can be concluded from this study:

(i) Controlling electron beam welding parameters when joining AA1350 aluminum alloy could produce high weldment strength and a narrow HAZ.

(ii) The UTS of the welded joint obtained by EBW technique can attain more than 90% of the strength of the unwelded base metal in this category of aluminum alloy having poor weldability.

(iii) The bead region in EBW joint demonstrates the lowest value of hardness relative to the strain hardened base metal due to the processes of crystallization and recrystallization during the advance of the localized electron beam.

(iv) The impact toughness of EBW joint can attain about 80% of the toughness of the base metal.

(v) The uses of the OVAT method are economical in run size and can greatly simplify the effect of the process parameter on the weldment strength. However OVAT design does not give precise information about interactions between parameters. A good alternative to the OVAT design is the factorial design, where tests are conducted at as many as possible combinations of the operating factors.

References:

[1] Wajira Mirihanage and Nanda Munasinghe *Modification of AA 5083 weld joint characteristics*, International Symposium of Research Students on Materials Science and Engineering, December 2004, Chennai, Ind

[2] Gene Mathers, *The welding of aluminium and its alloys*, Woodhead Publishing Ltd,2002,

[3] George E. Tot ten G. E. Totten & Associates, Inc. Seattle, Washington, U.S.A, *Handbook of Aluminum* Volume 1, Library of Congress, New York.

[4] Robert Bakish, editor, electron beam technology, John Wiley & Sons Inc., New York, 1962.

[5] Dasharath Ram, S. Sai Kumar and P.V. Moahan Ram, *MODELING AND OPTIMIZATION OF ELECTRON BEAM WELDING PROCESS USING ANOVA,* international Symposium of Research Students on Material Science and Engineering December 20-22, 2004, Chennai, India.

[6] Hidetoshi Fujii, Hideaki Umakoshi, Yasuhiro Aoki, Kiyoshi Nogi, *Bubble formation in aluminium alloy during electron beam welding*, Journal of Materials Processing Technology, 2004

[7] Hidetoshi Fujii, Kiyoshi Nogi, *Formation and disappearance of pores in aluminum alloy molten pool under microgravity*, Science and Technology of Advanced Materials 5 (2004)

[8] S. Malarvizhi, K. Raghukandan., N. Viswanathan, *fatigue behaviour of post weld heat treated electron beam welded AA2219 aluminum alloy joints, Material and design,* ScienceDirect, 2008.

[9] Daniel D. Frey, Fredrik Engelhardt, Edward M. Greitzer, *A role for "one-factor-at-a-time" experimentation in parameter design, Research in Engineering Design 14*

[10] M. I. Hussain, Z. M. Zain & M. S. Salleh, *Methodology of Designing Statistical Design of Experiment (SDE) to Study Wrinkles and Delamination on Composite Panels*, Journal of Quality and Technology Management Volume V, Issue I1, Dec, 2009,

[11] Jyh-Horng Choua, Shinn-Horng Chenb, Jin-Jeng Li, *Application of the Taguchi-genetic method to design an optimal grey-fuzzy controller of a constant turning force system*, Journal of Materials Processing Technology 105 (2000)

[12] Robert L. Mason, Richard F. Gunst, James L. Hess, *Statistical Design and Analysis of Experiments With Applications to Engineering and Science*, Second Edition, John Wiley & Sons, Inc, 2003

[13] Gary F. Benedict, *nontraditional manufacturing processes*, Marcel Dekker, New York 1987.